RSC Advances

c1ra00198a

PAPER

Adsorption of proteins to thin-films of PDMS and its effect on the adhesion of human endothelial cells

Karin Y. Chumbimuni-Torres, Ramon E. Coronado, Adelphe M. Mfuh, Carlos Castro-Guerrero, Maria Fernanda Silva, George R. Negrete, Rena Bizios and Carlos D. Garcia*

Nanostructured films of PDMS were fabricated and used to investigate protein adsorption and adhesion of human epithelial cells

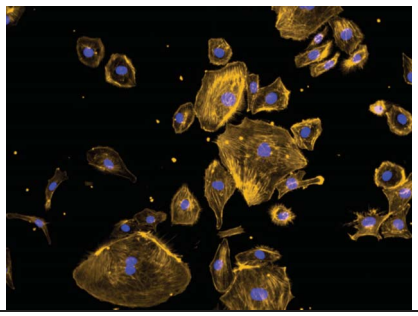

Please check this proof carefully. Our staff will not read it in detail after you have returned it.
Translation errors between word-processor files and typesetting systems can occur so the whole proof needs to be read. Please pay particular attention to: tabulated material; equations; numerical data; figures and graphics; and references. If you have not already indicated the corresponding author(s) please mark their name(s) with an asterisk. Please e-mail a list of corrections or the PDF with electronic notes attached — do not change the text within the PDF file or send a revised manuscript.

Please bear in mind that minor layout improvements, e.g. in line breaking, table widths and graphic placement, are routinely applied to the final version.

We will publish articles on the web as soon as possible after receiving your corrections; no late corrections will be made.

Please return your **final** corrections, where possible within **48 hours** of receipt, by e-mail to: advances@rsc.org

Electronic (PDF) reprints will be provided free of charge to the corresponding author. Enquiries about purchasing paper reprints should be addressed via: http://www.rsc.org/publishing/journals/guidelines/paperreprints. Costs for reprints are below:

Reprint costs

No of pages	Cost for 50 copies	Cost for each additional 50 copies
2–4	£225	£125
5–8	£350	£240
9–20	£675	£550
21–40	£1250	£975
>40	£1850	£1550

Cost for including cover of journal issue:
£55 per 50 copies

Authors Queries

Journal:

Paper: **c1ra00198a**

Title: **Adsorption of proteins to thin-films of PDMS and its effect on the adhesion of human endothelial cells**

Editor's queries are marked like this... [1], and for your convenience line numbers are indicated like this... 5.

Query Reference	Query	Remarks
1	[INFO-1] For your information: You can cite this paper before the page numbers are assigned with: (authors), RSC Adv., DOI: 10.1039/c1ra00198a.	
2	Please indicate what ??? signifies	

RSC Advances

Dynamic Article Links

Cite this: DOI: 10.1039/c1ra00198a

www.rsc.org/advances

PAPER

Adsorption of proteins to thin-films of PDMS and its effect on the adhesion of human endothelial cells†

Karin Y. Chumbimuni-Torres,[a] Ramon E. Coronado,[b] Adelphe M. Mfuh,[a] Carlos Castro-Guerrero,[c] Maria Fernanda Silva,[d] George R. Negrete,[a] Rena Bizios[b] and Carlos D. Garcia*[a]

Received 23rd May 2011, Accepted 22nd July 2011
DOI: 10.1039/c1ra00198a

This paper describes a simple and inexpensive procedure to produce thin-films of poly(dimethylsiloxane). Such films were characterized by a variety of techniques (ellipsometry, nuclear magnetic resonance, atomic force microscopy, and goniometry) and used to investigate the adsorption kinetics of three model proteins (fibrinogen, collagen type-I, and bovine serum albumin) under different conditions. The information collected from the protein adsorption studies was then used to investigate the adhesion of human dermal microvascular endothelial cells. The results of these studies suggest that these films can be used to model the surface properties of microdevices fabricated with commercial PDMS. Moreover, the paper provides guidelines to efficiently attach cells in BioMEMS devices.

1. Introduction

Recent developments in fabrication procedures and instrumentation[1] have enabled the development and application of microfluidic devices to chemical, biomedical,[2,3] pharmaceutical,[4] environmental, and forensic sciences.[5] Among other advantages, these devices have the potential to combine sample-handling capabilities, custom design, low-power requirements, and portability while providing similar performance to their standard bench-top counterparts. Additionally, various well-established laboratory techniques can be easily integrated in microfluidic devices, increasing the versatility and throughput of these systems.[6]

Although microfluidic devices were initially constructed using glass, a wide variety of polymeric materials have been recently used.[7–10] Among them, poly(dimethylsiloxane) (PDMS) has been one of the most widely used materials because it allows rapid fabrication of devices using relatively simple and inexpensive instrumentation.[11–14] Although the general attributes of PDMS and their molecular bases were recognized many decades ago,[15] it is worth highlighting its chemical inertness, low electrical conductivity, elasticity,[6] and optical transparency.[7,16] PDMS does not swell or dissolve in a number of solvents[17] and is permeable to most gases, including oxygen.[18] Despite several advantages of PDMS for microfluidic devices, several drawbacks still limit the applicability of this material.[19] Probably one of the most noteworthy characteristics of PDMS is its hydrophobic nature (contact angle ~110°) and porosity, allowing the absorption[20,21] and adsorption[22] of a wide variety of molecules. Because such processes can have negative effects in devices used for separations,[23,24] several procedures have been developed to control the surface properties of PDMS.[25–28] Taking advantage of the low surface energy of PDMS,[15] similar procedures have been used to produce patterns and arrays by exposing the surface of this material to target proteins.[29–34] In this regard, controlling not only the amount of adsorbed protein, but also the orientation and conformation of the protein layer is particularly important when proteins (such as fibronectin[35]) mediate interactions with other biological entities such as cells.[36–40] Despite the advantages and the intriguing nature of the studies reported in literature, only few research groups[41,42] have investigated the influence of adsorption kinetics on the biological activity of proteins adsorbed to PDMS. Because the adsorption rate can have a significant influence on the conformation and subsequent biological activity of the adsorbed protein layer, obtaining such information is critical to rationally design micro-electro mechanical systems for biological applications (BioMEMS).

For the aforementioned reasons, and aiming to address this gap in knowledge, thin-films of two *n*-dimethylsiloxanes were deposited on silicon substrates and characterized by a variety of complementary techniques. This approach developed to deposit thin-films of PDMS proved to be simpler and faster than others previously reported,[22,43–47] some of which did not render uniform layers of PDMS and thus were incompatible with ellipsometric measurements. The deposited thin-films, that have identical chemical composition and similar macroscopic properties than

[a]*Department of Chemistry, The University of Texas at San Antonio, TX, 78249, USA. E-mail: carlos.garcia@utsa.edu; Tel: (210) 458-5774*
[b]*Department of Biomedical Engineering, The University of Texas at San Antonio, San Antonio, USA*
[c]*Department of Physics and Astronomy, The University of Texas at San Antonio, San Antonio, USA*
[d]*School of Agronomic Sciences - IBAM-CONICET, National University of Cuyo, Mendoza, Argentina*
† Electronic Supplementary Information (ESI) available. See DOI: 10.1039/c1ra00198a/

commercial PDMS (*e.g.*, Sylgard 184), were then used to investigate the adsorption kinetics of three model proteins: fibrinogen (Fib), collagen type I (Col), and bovine serum albumin (BSA) under different protein concentrations and pH values. Spectroscopic ellipsometry was used to characterize the optical properties of the films and to follow the adsorption process of each protein in real time. Finally, the selected substrates were used to evaluate the role of the characterized adsorbed protein layer on the adhesion and morphology of human dermal endothelial cells.

2. Experimental

2.1. Reagents and solutions

All chemicals were analytical reagent grade and used as received. Hydrogen peroxide, sodium hydroxide, and sodium dodecyl sulfate (SDS) were purchased from Fisher Scientific (Fair Lawn, NJ). All aqueous solutions were prepared using 18 MΩ cm water (NANOpure Diamond, Barnstead; Dubuque, IA). The pH of the solutions was adjusted using either 1 M NaOH or 1 M HCl and measured using a glass electrode and a digital pH meter (Orion 420A+, Thermo; Waltham, MA). Two chlorine-terminated *n*-dimethylsiloxanes were selected for these studies: 1,3-dicholoro-1,1,3,3-tetramethyldisiloxane (n = 2) and 1,7-dicholoro-octamethyltetrasiloxane (n = 4). These chemicals were purchased from Sigma-Aldrich (St. Louis, MO) and used as received. Dichloromethane (DCM) was also purchased from Sigma Aldrich and isopropanol (analytical grade) was obtained from Fisher Scientific. Unless otherwise stated, solutions of either bovine serum albumin (Fraction V, Fisher Scientific) or fibrinogen (Fraction I, type 1-S from bovine plasma, Sigma-Aldrich) were prepared in 10 mM phosphate buffer pH = 7.0. Collagen type-I (from rat tail) was purchased from Invitrogen (Grand Island, NY) and dissolved in acetate buffer (0.04 M, pH = 4.8) following manufacturer's instructions, ensuring complete dissolution. The most relevant properties of the chosen proteins are summarized in Table 1. Isoelectric points (IEP) were obtained from the literature. Data related to the temperature at which the denaturation transition is half completed (T_m) were also obtained from the literature and included to provide information regarding the structural stability of the chosen molecules in comparison to the control protein, BSA (which is typically considered a *soft* protein prone to denaturation upon adsorption).[48,49] Unless otherwise stated, all experiments were conducted at room temperature (22 ± 1 °C).

2.2. Synthesis and characterization of nanostructured films

Standard <111> silicon wafers (Si/SiO_2, Sumco; Phoenix, AZ) were initially scored using a computer-controlled engraver (Gravograph IS400, Gravotech; Duluth, GA). The process defined substrates of 1 cm in width and 3 cm in length that were then manually cut and cleaned in piranha solution (30% hydrogen peroxide and 70% sulfuric acid) at 90 °C for 30 min. After thorough rinsing with water, the substrates were immersed and stored in ultrapure water until use. In order to deposit the thin-films on the substrates, the clean wafers were dried at 80 °C for 4 h and immersed in solutions containing the corresponding *n*-dimethylsiloxane (dissolved in dichloromethane) for 3 h, under gentle stirring (100 rpm; Innova 2000; New Brunswick Sci.). Subsequently, the coated wafers were sequentially rinsed with isopropanol and water, dried in a convection oven, and stored until use. Under the selected conditions, the attachment reaction proceeds rather quickly leading to the deposition of a layer of *n*-dimethylsiloxane covalently linked to the substrate by a head-to-surface arrangement.[53,54]

Films produced by the deposition reaction of 1,7-dicholoro-octamethyltetrasiloxane were characterized by nuclear magnetic resonance (^{1}H-NMR and ^{13}C-NMR in $CDCl_3$) using a Varian INOVA 500 MHz Spectrometer. For comparison purposes, the ^{1}H-NMR of 1,7-dicholoro-octamethyltetrasiloxane was also obtained in $CDCl_3$. In order to analyze the reaction products, silica beads (>15 nm) were modified with 1,7-dicholoro-octamethyltetrasiloxane, suspended in $CDCl_3$, and analyzed under conditions similar to those of the precursors in solution.

Contact angle measurements, used to evaluate the surface hydrophobicity of the prepared substrates, were performed using a VCA-Optima surface analysis system (Ast Products, Inc.; Billerica, MA) and analyzed using the software provided by the manufacturer, 30 s after dispensing 2 μL of deionized water. Atomic force microscopy (AFM) images were obtained using a Veeco diMultiMode Nanoscope V scanning probe microscope operating in tapping and non-contact mode. The samples were analyzed without any coating.

2.3. Spectroscopic ellipsometry

Experiments were performed using a variable angle spectroscopic ellipsometer (WVASE, J.A. Woollam Co., Lincoln, NE) following a procedure described elsewhere.[55–58] Under these conditions, spectroscopic ellipsometry has proven suitable to study the kinetics of protein adsorption processes[59] and to calculate the optical constants, thickness, and microstructure of the adsorbed film. The sensitivity of the technique, critically evaluated elsewhere,[60] was also considered appropriate for the purpose of the present study. Collected data (ellipsometric angles as function of time, angle, and/or wavelength) were modeled using the WVASE software package (J. A. Woollam Co., Lincoln, NE). Differences between the experimental and model-generated data were assessed by the mean square error (MSE),[61] a built-in function in WVASE based on eqn (2),

$$MSE = \frac{1}{2N-M}\sum_{i=1}^{N}\left[\left(\frac{\Psi_i^{\mathrm{mod}}-\Psi_i^{\mathrm{exp}}}{\sigma_{\Psi,i}^{\mathrm{exp}}}\right)^2+\left(\frac{\Delta_i^{\mathrm{mod}}-\Delta_i^{\mathrm{exp}}}{\sigma_{\Delta,i}^{\mathrm{exp}}}\right)^2\right] = \frac{1}{2N-M}X^2 \quad (2)$$

where N is the number of Ψ and Δ pairs used in the measurement, M is the number of parameters varied in the regression analysis, and σ is the standard deviation of the experimental data

Table 1 Most relevant properties of the proteins selected for these studies

Protein	MW (KDa)	Dimensions (nm)	IEP	T_m (°C)	Ref.
BSA	66.5	14 × 4 × 4 (heart)	4.8	57	50
Fib	340	47 × 4.5 (trinodular)	5.5	53	51
Col	300	300 × 1.5 (rod)	7.8	38	52

points. Although smaller MSE values indicate better fittings, MSE < 10 are typically considered acceptable.

Before each protein adsorption experiment, the thickness of the deposited layer was measured by placing the substrate in the ellipsometry cell[59] and by performing a spectroscopic scan in the 300 to 800 nm range (with 10 nm steps) using the corresponding aqueous buffer as the ambient medium. Then, the dynamic experiment was initiated by pumping background electrolyte through the cell at a rate of 1 mL min^{-1} to establish the baseline. Next, the protein solution was introduced, and the adsorption process initiated. An initial fast process, followed by a slower one, was always observed. After a plateau in the signal was observed, the dynamic scan was stopped, and a spectroscopic scan was collected to verify the thickness of the adsorbed protein layer. Experiments performed in this way provided data for calculating the initial protein adsorption rate and the saturation amount. Subsequently to protein adsorption, a desorption experiment was performed using the corresponding buffer ($\sim$10 min) and then 4 mmol L^{-1} SDS (30 min). In between experiments, the flow cell and tubing were thoroughly rinsed (with 0.1 mM SDS and water) to avoid cross-contamination.

2.4. Optical models

One of the limitations of ellipsometry is the requirement for an optical model that describes the properties of the substrates in terms of optical constants (refractive index, n, and extinction coefficient, k) and thickness (d).[62] In the present study, the model used to represent the optical properties of the substrates was composed of a layer of Si (bulk; d = 1 mm), a layer of SiO_2 (d = 2.5 $\pm$ 0.5 nm), and a transparent layer (representing the n(dimethylsiloxane) film), represented by a Cauchy function (eqn (1)),

$$n_{(\lambda)} = A + \frac{B}{\lambda^2} + \frac{C}{\lambda^4} \quad (1)$$

where λ is the wavelength and A, B, and C are computer generated fitting parameters.[63] In agreement with previous experiments performed under similar conditions,[55,59,60,64] adsorbed proteins were represented by an additional layer (described with an additional Cauchy function) where A = 1.465, B = 0.01, and C = 0. These parameters yielded index of refraction values ranging from 1.527 to 1.477, which are consistent with previously reported values for other adsorbed proteins.[65,66] Under the chosen experimental conditions, ellipsometry can be used to determine the amount of adsorbed protein (Γ, expressed in mg m^{-2}) using eqn (2),

$$\Gamma = \frac{d(n - n_0)}{(dn/dc)} \quad (2)$$

where n and n_o are the refractive index of the protein and of the ambient (aqueous buffer), respectively.[67] In accordance with previous reports,[68–71] the refractive index increment for the proteins in the adsorbed layer (dn/dc) was assumed to be 0.187 mL g^{-1}.

2.5. Cell culture, cell adhesion and cell morphology experiments

Human dermal microvascular endothelial cells (HDMEC) were purchased from Sciencell (Carlsbad, CA) and cultured under standard conditions (*i.e.*, a humidified, 37 °C, 5% CO_2/95% air environment) in endothelial-cell complete medium (Sciencell; the composition and concentration of the supplements contained in this complete medium are proprietary vendor information). When confluent, the cells were passaged after a short (6 min) exposure to a trypsin/EDTA solution (BioCell; Rancho Dominguez, CA), and re-suspended in fresh serum-free basal endothelial-cell media (without supplements). Cells at passage number 3 were used for the experiments.

For these studies, substrates (1 cm $\times$ 1 cm) were modified with 1,7-dicholoro-octamethyltetrasiloxane according to the described procedure and then immersed (under constant agitation at 100 rpm) in solutions containing each one of the proteins tested under the chosen experimental conditions for two hours. Next, the protein-modified substrates were thoroughly rinsed with buffer (to remove loosely-bound proteins) and placed one each in individual wells of polystyrene tissue-culture plates (12-wells/plate, 22.1 mm internal diameter).

Human dermal microvascular endothelial cells were seeded (48 000 cells/well containing one substrate) in Dulbecco's Phosphate Buffered Saline with neither calcium nor magnesium (DPBS) and allowed to interact for 3 h. The adhered cells were then fixed *in situ* using 4% formaldehyde in DPBS for 15 min, rinsed twice with fresh DPBS, treated with 0.1% Triton-X, and finally stained with Alexa Fluor 568® Phalloidin (to visualize the F-actin filaments of the cytoskeleton) and/or 4′,6-diamidino-2-phenylindole dilactate (DAPI) (to visualize the cell nuclei). Both fluorescent stains were purchased from Invitrogen (Carlsbad, CA) and were used following procedures provided by the vendor. A fluorescent microscope (LEICA DM 5500B) was used to visualize the F-actin filaments (excitation/emission of 578/600 nm, respectively) and the cell nuclei (excitation at 358 nm/emission at 461 nm). All experiments were run in duplicate and repeated at three separate times. In all cases, 20 micrographs/sample were examined to determine adhering cell morphology and number of attached cells.

3. Results and discussion

3.1. Characterization of nanofilms

An optical model was developed to represent the optical properties of the substrates and to interpret the adsorption experiments. In all cases, a very good agreement (MSE < 10) between the experimental and the model-calculated data was obtained, indicating that the proposed model enables the description of the properties of the substrates and that it can be used to calculate thickness of the films. As a representative example, Fig. 1A shows the data collected during a spectroscopic scan (dependence of Ψ and Δ as a function of λ) obtained at three different angles of incidence for a thin-film of PDMS (fabricated from the reaction of 1,7-dicholoro-octamethyltetrasiloxane). Fig. 1A also shows the data generated using the corresponding optical model. As can be observed, a very good agreement (MSE < 5) between the experimental (data points) and the model-generated data (lines) was obtained. The optical constants calculated form these experiments (data not shown) are also in agreement with previously reported values for PDMS,[72] though measured in a narrower spectral interval.

Additionally, reflective UV-Vis spectra (R_P and R_S; data not shown) confirmed the presence of a transparent film (measured in the 250–800 nm range) with isotropic properties, also in good

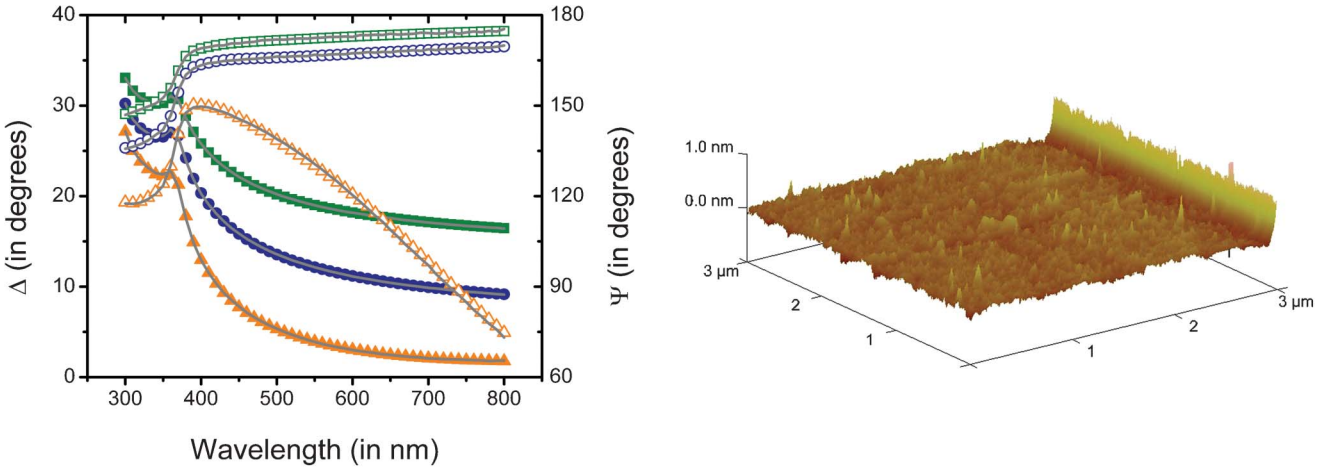

Fig. 1 A: Spectroscopic scans corresponding to data experimentally collected (points) and calculated with the optical model (lines) corresponding to a Si/SiO_2 substrate coated with a thin-film of PDMS of 2.01 ± 0.02 nm (MSE=4.3) fabricated from the reaction of 1,7-dicholoro-octamethyltetrasiloxane. Ψ and Δ values are represented with solid and open symbols, respectively. Angle of incidence: 65° (??? and ???), 70° (??? and ???), and 75° (??? and ???). B: 3D AFM image corresponding to a Si/SiO_2 substrate coated with a thin-film of PDMS of 2.01 ± 0.02 nm fabricated from the reaction of 1,7-dicholoro-octamethyltetrasiloxane.

agreement with the optical properties of PDMS.[73,74] Furthermore, the aforementioned optical model also allowed calculation of the thickness of the *n*-dimethylsiloxane films deposited on the Si/SiO_2 substrates. According to our results, treating the Si/SiO_2 wafers with either 1,3-dicholoro-tetramethyl-disiloxane or 1,7-dicholoro-octamethyltetrasiloxane produced uniform films with average thickness values of 1.3 ± 0.1 nm and 2.1 ± 0.2 nm (n = 3, independently prepared), respectively. Because the molecular dimensions of *di-* and *tetra*-(dimethyl-siloxane) were calculated to be 0.65 and 1.33 nm, respectively (see ESI†) our results suggest that in both cases, the films are constituted by entangled oligomers (dimers and/or trimers) of the corresponding *n*-dimethylsiloxane covalently linked to the surface. Such arrangement closely resembles the porous structure of commercial PDMS. This conclusion is in good agreement with reports in the literature stating that many of the properties of PDMS are consequence of the static and dynamic structure of the siloxane backbone[75] and the hydrophobicity of the methyl chain.[76] In the case of the present study, these properties are indistinguishable from those of commercial PDMS. Also in agreement with previously reported values for commercial PDMS,[77] the contact angle of the deposited films was 114 ± 2° (n = 3, independently prepared), indicating the presence of a rather hydrophobic surface. Furthermore, the topography of the substrates was investigated by atomic force microscopy (see representative image in Fig. 1B) and showed the presence of a smooth film on the silica wafer with abundant nanostructured features on the surface. The size of those features (as calculated form the roughness of the AFM images) was 0.2 ± 0.1 nm.

Films made with 1,3-dicholoro-1,1,3,3-tetramethyldisiloxane and 1,7-dicholoro-octamethyltetrasiloxane were then used to evaluate the dynamic adsorption of fibrinogen (0.1 mg mL^{-1} in 10 mM PBS, pH = 7.7). An unmodified wafer (Si/SiO_2) was used as a control surface. According to our results (data not shown), fibrinogen attached onto both films and to the silica surface with almost identical initial adsorption rates (dΓ/dt), reaching Γ_{SAT} values of 3.6 ± 0.1 mg m^{-2} and 3.4 ± 0.1 mg m^{-2}, respectively. Rinsing the samples with buffer did not induce desorption of fibrinogen from the substrate surfaces tested. It was also observed that, while SDS induced desorption of 81% of the fibrinogen adsorbed onto Si/SiO_2, a much smaller fraction (27% and 13%) was removed from the substrate surfaces coated with either 1,3-dicholoro-1,1,3,3-tetramethyldisiloxane or 1,7-dicholoro-octamethyltetrasiloxane, respectively. In line with previous reports,[58,78] our results show that the three surfaces tested exhibited high fibrinogen adsorption, regardless of whether the surface was hydrophilic or hydrophobic.[79] However, the binding strength of fibrinogen (as measured by elutability with SDS[80–83]) was significantly higher on the dimethylsiloxane-treated surface than on the plain silica surface. These results also support the hypothesis that 1,7-dicholoro-octamethyltetrasiloxane can coat the silica surface with a coverage higher than that of the 1,3-dicholoro-1,1,3,3-tetramethyldisiloxane, explaining the intermediate behavior observed during the protein desorption studies performed with SDS. Consequently, films made with 1,7-dicholoro-octamethyltetrasiloxane were considered more suitable for the scope of the present project, were further characterized, and used for the rest of the experiments described in the present manuscript. These films will be referred to as PDMS-like films for the remaining part of this paper.

NMR was used to gain insight on the structures of both the precursor and the deposited films (data included as ESI†). Two signals of identical intensity were observed for the precursor (1,7-dicholoro-octamethyltetrasiloxane): the signal observed at 0.14 ppm was assigned to the protons on the methyl groups attached to internal Si atoms, while the signal that appeared downfield (0.46 ppm) was assigned to the protons on the methyl groups in the vicinity of the chlorinated terminal Si atoms. In order to analyze the products of the reaction between the selected n-dimethylsiloxanes and silica by NMR, the glass inner surface of the NMR tube was modified according to the previously described procedure. However, the magnitude of the obtained signal was not considered appropriate. Consequently and aiming to increase the amount of material available, silica

beads were modified with 1,7-dicholoro-octamethyltetrasiloxane under conditions identical to those used to modify the Si/SiO_2 wafers, suspended in $CDCl_3$ and analyzed using standard procedures. It is worth mentioning that a single peak (at 1.50 ppm) was observed in the ^{1}H-NMR of the plain beads and was attributed to the protons in the SiOH groups of the surface. Conversely, the ^{1}H-NMR of the modified beads showed a main peak (at 0.05 ppm), and a series of much smaller peaks at 1.57 and 4.84 ppm. The signal observed at 4.84 ppm was a rather small and broad peak, characteristic of protons in groups linked to surfaces. As expected, the ^{13}C-NMR of the modified beads displayed a main peak at 1.00 ppm and a smaller peak at 0.74 ppm. Although a detailed description of the chemical connectivity of the deposited film was not possible from these experiments, the relative intensity of the peaks clearly demonstrates the presence of hydrogen and carbon atoms, therefore confirming the possibility to attach methyl groups to the silica surface.

Adsorption of proteins onto PDMS-like films. Three model proteins were selected for the present studies: bovine serum albumin (BSA), fibrinogen (Fib) and collagen type-I (Col). BSA was chosen as control protein, because it blocks the adsorption of other proteins and the adhesion of cells. Collagen[84] and fibrinogen[51,85] were selected because of their biomedical relevance. Specifically, Collagen I is a major adhesive protein in the extracellular matrix of many tissues while Fib has a crucial role in the blood coagulation process. Fig. 2 shows representative results of the dynamic adsorption experiments for BSA (in 10 mM PBS at pH = 7.0), fibrinogen (in 50 mM PBS at pH = 7.7) and collagen (in acetate buffer 40 mM at pH = 4.8), each one at a concentration of 0.01 mg mL^{-1} onto the thin-films of PDMS.

These experimental conditions were chosen to ensure complete dissolution of the proteins and to allow comparison of the results of the present studies with others reported for BSA,[50] fibrinogen,[86] and collagen[84]. The first noticeable aspect is that, despite having the highest molecular weight, fibrinogen adsorbed to the substrate surface at the highest rate (0.33 $\pm$ 0.02 mg m^{-2} min^{-1}). This result suggests that interactions with the substrate surface (and not only the flux of protein) played a fundamental role in the adsorption rate of Col and BSA. Conversely, it is important to note that the highest adsorbed amount of protein was obtained with collagen (2.6 $\pm$ 0.1 mg m^{-2}). These results can be attributed to a combination of favorable electrostatic interactions (surface-to-protein) and slow rearrangements in the adsorbed layer. Probably the most important conclusion that can be extracted from these results is that similar conditions shall not be used if equivalent films of fibrinogen and collagen are to be adsorbed. While 82% of the saturation amount (Γ_{SAT}) of fibrinogen can be achieved in 40 min, only 35% of the Γ_{SAT} of collagen was adsorbed to the substrate surface during that period of time. This is a critical aspect to consider when adsorbing proteins because typically, there is a dynamic competition between the adsorption process and the structural rearrangements of the protein at the surface. While the former process increases the number of proteins adsorbed per unit area; the latter allows proteins to relax, maximize the interaction with the substrate surface, and leads to significant reductions in biological activity.

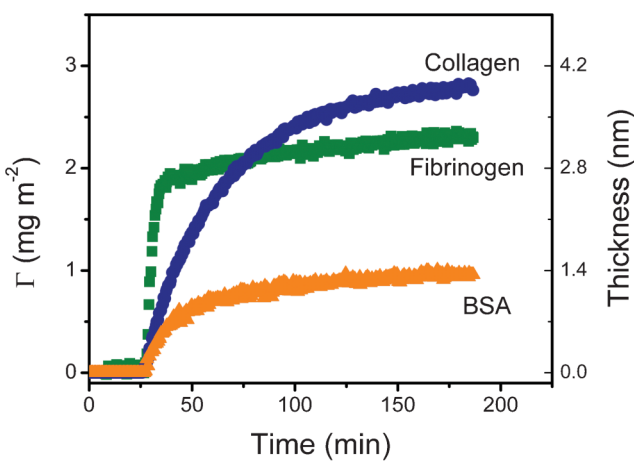

Fig. 2 Dynamic adsorption experiments of BSA (in 10 mM PBS at pH = 7.0), fibrinogen (in 50 mM PBS at pH = 7.7) and collagen (in acetate buffer 40 mM at pH = 4.8) at a concentration of 0.01 mg mL^{-1} onto the nanostructured films.

Considering the dimensions and structural rigidity of the selected proteins (Table 1) as well as the average thickness of the protein layers adsorbed onto the PDMS-like surface, it is reasonable to consider that, while BSA and fibrinogen formed a single (most likely incomplete) layer[85,87,88] with side-on arrangement, collagen formed an entangled multilayer of linear fibers.

The effect of protein concentration on the adsorbed amount (Γ) onto the PDMS-coated surfaces was investigated in real-time for the three chosen proteins. The representative example of Fig. 3A shows the results obtained for fibrinogen. It was observed that both the amount of adsorbed fibrinogen and the initial adsorption rate increased as function of protein concentration. It is also interesting to note that, a secondary process was observed (at $\sim$60 min) when fibrinogen at 0.1 mg mL^{-1} was used, suggesting that post-adsorption re-arrangements (from side-on to head-on) may be occurring. This observation is also in agreement with a molecular area of 2.4 mg m^{-2} of fibrinogen in a closely packed monolayer with side-on configuration, reported by Wertz and Santore.[87] Post-adsorption processes such as *tilting*, *rolling*, and *spreading* have been reported for a number of proteins[89–91] (including fibrinogen[85,92,93]) and are relevant because they may significantly affect the biological activity of the adsorbed molecules.

The amount of fibrinogen adsorbed on the PDMS film as a function of time and in response to changes in the pH of the buffer solution was also determined using spectroscopic ellipsometry. For these experiments, four pH values were selected taking into consideration the isoelectric point of each protein (Table 1). These experiments enabled evaluation of the relative contribution of electrostatic and hydrophobic forces on the interaction of proteins with both the surface and the proteins already adsorbed to the substrate surface. Altering the charge of fibrinogen (0.01 mg mL^{-1}) by changing the pH of the buffer solution affected protein adsorption onto the PDMS-like substrate (Fig. 3B). In all cases, a significant increase on the amount of protein adsorbed was observed as the solution pH approached the isoelectric point of each protein. Similarly, the initial adsorption rate was fastest at pH values around the isoelectric point of each protein tested but decreased as the pH of the solution moved further away from the isoelectric point of

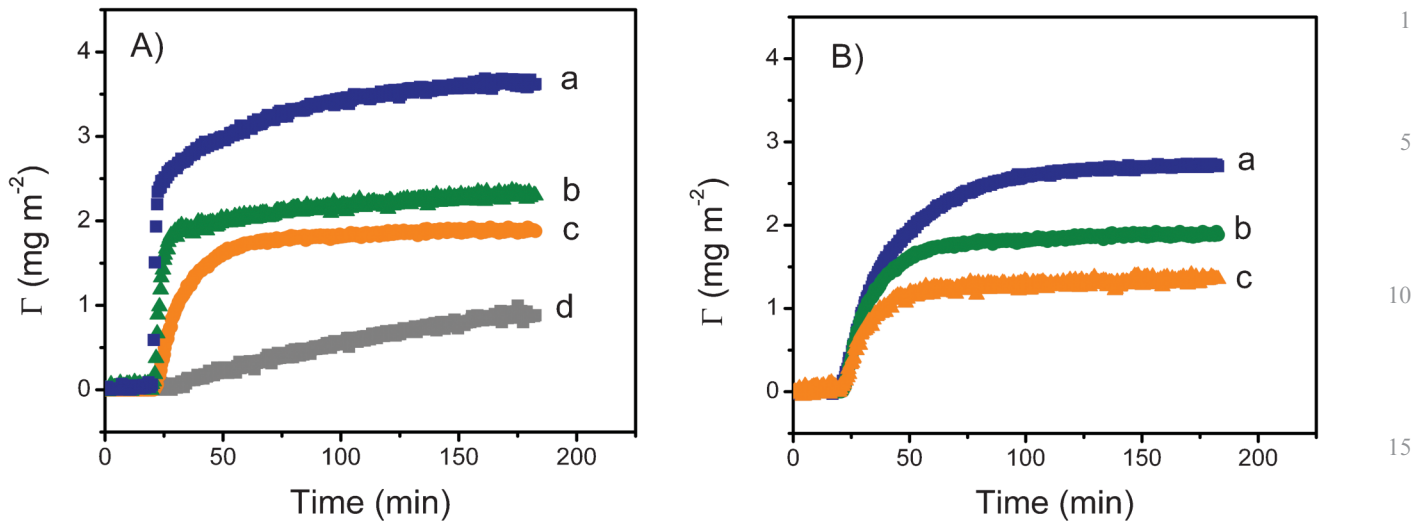

Fig. 3 A: Effect of protein concentration on the dynamic adsorption of fibrinogen onto PDMS-like nanofilms. Conditions: (a) 0.1 mg mL^{-1}, (b) 0.01 mg mL^{-1}, (c) 0.001 mg mL^{-1} and (d) 0.0001 mg/mL. B: Effect of pH on the dynamic adsorption of fibrinogen (0.01 mg mL^{-1}) onto PDMS-like nanofilms. Conditions: (a) pH = 6.6, (b) pH = 7.7 and (c) pH = 8.7.

each protein. The results of the adsorption studies for the three selected proteins are summarized in Table 2.

The experiments of the present study provided unique insights into the amount and arrangement of proteins adsorbed onto the thin-films of PDMS. In agreement with literature reports, the highest amount of protein was adsorbed when the pH of the buffer solution was close to, or near, the isoelectric point of the respective protein. This observation is in agreement with literature reports stating that, due to minimal protein-to-protein electrostatic interactions, higher protein adsorption rates are usually observed at the IEP.[49,94,95] When compared to results calculated from a purely diffusion-limited model,[59] these results indicate that the attachment to the surface plays a fundamental role in the adsorption of the selected proteins. For that reason, maximizing the adsorption rate has proven to be an effective way to minimize structural rearrangements (such as spreading) of the adsorbing protein molecules. In addition, measurements of the initial adsorption rate only require a small amount of protein and can be completed in a relatively short timescale (~20 min). On the other hand, measurements of the saturation amount can take significantly longer, allowing post-adsorption processes to influence the interpretation of the observed phenomena.

The importance of hydrophobic interactions in the adsorption of the chosen proteins is evidenced by the strong adsorption observed even under unfavorable electrostatic interactions. The results of the present study provide guidelines to assist other researchers to select the most favorable and time-efficient conditions to adsorb proteins onto PDMS.

Table 2 Kinetic data and adsorption conditions of proteins onto PDMS-like films

	Adsorption conditions			
Protein	Concentration	pH	$d\Gamma/dt$ (mg m^{-2} min^{-1})	Γ_{SAT} (mg m^{-2})
BSA	0.1	7.0	0.21 ± 0.03	1.3 ± 0.1
	0.01	7.0	0.06 ± 0.01	1.0 ± 0.2
	0.001	7.0	0.006 ± 0.005	0.4 ± 0.1
Fib	0.1	7.7	1.03 ± 0.11	3.6 ± 0.2
	0.01	7.7	0.445 ± 0.06	2.3 ± 0.2
	0.001	7.7	0.07 ± 0.02	1.9 ± 0.3
	0.0001	7.7	0.01 ± 0.01	0.89 ± 0.09
	0.001	8.7	0.04 ± 0.004	1.35 ± 0.2
	0.001	6.7	0.08 ± 0.008	2.7 ± 0.2
Col	0.01	4.8	0.10 ± 0.01	2.70 ± 0.29
	0.001	4.8	0.04 ± 0.01	1.84 ± 0.11
	0.0001	4.8	0.01 ± 0.01	0.60 ± 0.08
	0.001	4.0	0.02 ± 0.01	0.92 ± 0.09

Cell adhesion and morphology onto protein-modified surfaces. The role of pre-adsorbed proteins on cell-adhesion and morphology was examined. For these experiments, the Si/SiO_2 substrates tested were first coated with 1,7-dicholoro-octamethyltetrasiloxane (to deposit a thin-film of PDMS of about 2 nm), and then modified by the adsorption of proteins. For each protein, two experimental conditions were selected as either favorable or unfavorable (based on the dynamic protein adsorption data). BSA, which does not mediate the adhesion of cells to substrates, was chosen as a reference. Table 3 summarizes the selected conditions for each protein.

In addition to unmodified silica substrates (Si/SiO_2), substrates coated with the thin-films of PDMS but without pre-adsorbed proteins were used as controls. Details of the procedures followed in evaluating cell adhesion and morphology are given in the Experimental section of this manuscript.

The results provided evidence that HDMEC adhered to all substrates tested. Although the number of adherent cells was

Table 3 Parameters selected to evaluate the effect of adsorption conditions on the adhesion of HDMEC

Protein	Favorable conditions	Unfavorable conditions
BSA	0.01 mg mL^{-1} PBS, pH = 7.0	0.0001 mg mL^{-1} PBS, pH = 7.0
Fib	0.01 mg mL^{-1} PBS, pH = 6.7	0.0001 mg mL^{-1} PBS, pH = 7.7
Col	0.01 mg mL^{-1} Acetate, pH = 4.8	0.0001 mg mL^{-1} Acetate, pH = 6.0

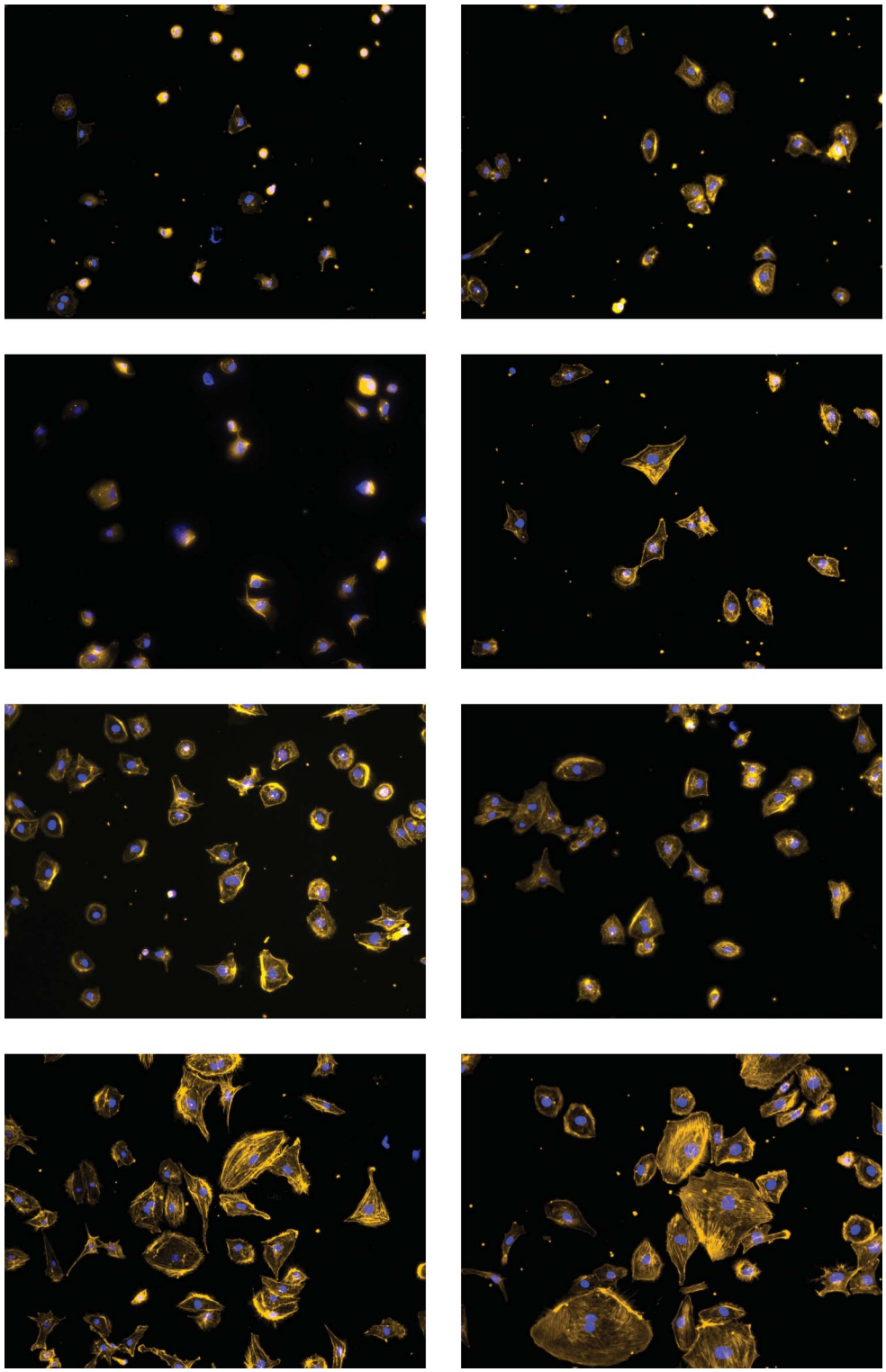

Fig. 4 Fluorescent micrographs of human dermal microvessel endothelial cells after 3 h of adhesion on the selected substrates. Stains: Alexa Fluor 568® Phalloidin and 4′′,6-diamidino-2-phenylindole dilactate. Magnification: 20×. (A) Si/SiO2 substrate; (B) Unmodified substrate coated with PDMS-like film; (C) PDMS-like substrate modified with BSA under favorable conditions; (D) PDMS-like substrate modified with BSA under unfavorable conditions; (E) PDMS-like substrate modified with Fib under unfavorable conditions; (F) PDMS-like substrate modified with Col under unfavorable conditions; (G) PDMS-like substrate modified with Col under favorable conditions; (H) PDMS-like substrate modified with Fib under favorable conditions.

similar on all the substrate surfaces of interest to the present study, significant differences in cell morphology were observed. Cells did not spread out when adhering onto the unmodified silicon substrate (Fig. 4A). Only slight spreading was observed when cells adhered onto the plain PDMS-like substrates or the substrates modified with BSA at either condition tested (Fig. 4B–D). In contrast, spread-out cells were observed on all other substrates tested; however, the degree of cell spreading was dependent on the type and amount of adsorbed protein. In this respect, adhered cells exhibited moderate spread-out morphology onto PDMS-like substrates modified with either collagen type-I or fibrinogen under unfavorable conditions (Fig. 4E–F). Cells adhering onto PDMS-like substrates modified with either collagen or fibrinogen under the most favorable conditions, exhibited the most spread-out cell morphology (Fig. 4G–H). In addition, the adherent cells exhibited the typical F-actin arrangement for endothelial cells, specifically, a concentric arrangement along the cell periphery as well as filaments transversing the cell cytoplasm.

4. Conclusions

This report described a simple procedure to fabricate films of n-dimethylsiloxane covalently attached to Si/SiO_2 substrates. The films were characterized by ellipsometry, ^{1}H-NMR, ^{13}C-NMR, contact angle measurements, and atomic force microscopy. According to the presented results, exposing the surface of SiO_2 to 1,7-dicholoro-octamethyltetrasiloxane leads to the deposition of homogeneous films of about 2 nm in thickness with characteristics similar to those of commercial PDMS. Dynamic adsorption experiments showed that the selected proteins (BSA, Fib, and Col) adsorbed onto the surface of the films with high affinity, that such adsorption process was determined by a combination of hydrophobic and electrostatic interactions, and that experimental conditions can be rationally selected to minimize protein spreading on the PDMS surface. Such knowledge of protein adsorption could lead to improved understanding of cell and tissue interactions on material surfaces pertinent to biomedical applications.

Acknowledgements

Financial support for this project was provided by the University of Texas at San Antonio and the National Institutes of Health through the National Institute of General Medical Sciences (1SC3GM081085) and the Research Centers at Minority Institutions (2G12RR013646-11). The authors would also like to thank J. L. Felhofer and M. Penick for helpful discussions.

References

1 J. L. Felhofer, L. Blanes and C. D. Garcia, *Electrophoresis*, 2010, **31**, 2469–2486.
2 J. R. Kraly, R. E. Holcomb, Q. Guan and C. S. Henry, *Anal. Chim. Acta*, 2009, **653**, 23–35.
3 Y. Xu, X. Yang and E. Wang, *Anal. Chim. Acta*, 2010, **683**, 12–20.
4 B. H. Weigl, R. L. Bardell and C. R. Cabrera, *Adv. Drug Delivery Rev.*, 2003, **55**, 349–377.
5 T. Vilkner, D. Janasek and A. Manz, *Anal. Chem.*, 2004, **76**, 3373–3386.
6 J. M. K. Ng, I. Gitlin, A. D. Stroock and G. M. Whitesides, *Electrophoresis*, 2002, **23**, 3461–3473.
7 H. Becker and L. Locascio, *Talanta*, 2002, **56**, 267–287.
8 M. Castano-Alvarez, M. T. Fernandez-Abedul and A. Costa-García, *Electrophoresis*, 2005, **26**, 3160–3168.
9 J. A. Vickers, B. M. Dressen, M. C. Weston, K. Boonsong, O. Chailapakul, D. M. Cropek and C. S. Henry, *Electrophoresis*, 2007, **28**, 1123–1129.
10 J. Liu, X. Sun and M. L. Lee, *Anal. Chem.*, 2007, **79**, 1926–1931.
11 C. D. García and C. S. Henry, in *Microchip Capillary Electrophoresis: Methods and Protocols*, ed. C. S. Henry, Humana Press, Totowa, NJ2006, pp. pp. 27–36..
12 M. Zhang, J. Wu, L. Wang, K. Xiao and W. Wen, *Lab Chip*, 2010, **10**, 1199–1203.
13 W. Schrott, M. Svoboda, Z. Slouka, M. Pribyl and D. Snita, *Microelectron. Eng.*, 2010, **87**, 1600–1602.
14 E. W. K. Young, E. Berthier, D. J. Guckenberger, E. Sackmann, C. Lamers, I. Meyvantsson, A. Huttenlocher and D. J. Beebe, *Anal. Chem.*, 2011, **83**, 1408–1417.
15 P. Zheng and T. J. McCarthy, *Langmuir*, 2010, **26**, 18585–18590.
16 D. K. Cai, A. Neyer, R. Kuckuk and H. M. Heise, *Opt. Mater.*, 2008, **30**, 1157–1161.
17 J. N. Lee, C. Park and G. M. Whitesides, *Anal. Chem.*, 2003, **75**, 6544–6554.
18 T. C. Merkel, V. I. Bondar, K. Nagai, B. D. Freeman and I. Pinnau, *J. Polym. Sci., Part B: Polym. Phys.*, 2000, **38**, 415–434.
19 R. Mukhopadhyay, *Anal. Chem.*, 2007, **79**, 3248–3253.
20 M. W. Toepke and D. J. Beebe, *Lab Chip*, 2006, **6**, 1484–1486.
21 K. Ren, Y. Zhao, J. Su, D. Ryan and H. Wu, *Anal. Chem.*, 2010, **82**, 5965–5971.
22 M. F. Mora, C. E. Giacomelli and C. D. Garcia, *Anal. Chem.*, 2007, **79**, 6675–6681.
23 H. Makamba, J. H. Kim, K. Lim, N. Park and J. H. Hahn, *Electrophoresis*, 2003, **24**, 3607–3619.
24 B. Huang, S. Kim, H. Wu and R. N. Zare, *Anal. Chem.*, 2007, **79**, 9145–9149.
25 F. Abbasi, H. Mirzadeh and A.-A. Katbab, *Polym. Int.*, 2001, **50**, 1279–1287.
26 I. Wong and C.-M. Ho, *Microfluid. Nanofluid.*, 2009, **7**, 291–306.
27 J. Zhou, A. V. Ellis and N. H. Voelcker, *Electrophoresis*, 2010, **31**, 2–16.
28 N. Maheshwari, A. Kottantharayil, M. Kumar and S. Mukherji, *Appl. Surf. Sci.*, 2010, **257**, 451–457.
29 G. Hu, Y. Gao, P. M. Sherman and D. Li, *Microfluid. Nanofluid.*, 2005, **1**, 346–355.
30 S. H. Chung and J. Min, *Ultramicroscopy*, 2009, **109**, 861–867.
31 L. Wang, L. Lei, X. F. Ni, J. Shi and Y. Chen, *Microelectron. Eng.*, 2009, **86**, 1462–1464.
32 L. Yu, *Nanotechnology*, 2009, **20**, 285101.
33 W. Zhang, C.-Y. Xue and K.-L. Yang, *J. Colloid Interface Sci.*, 2010, **353**, 143–148.
34 C. Volcke, R. P. Gandhiraman, L. Basabe-Desmonts, M. Iacono, V. Gubala, F. Cecchet, A. A. Cafolla and D. E. Williams, *Biosens. Bioelectron.*, 2010, **25**, 1295–1300.
35 G. K. Toworfe, R. J. Composto, C. S. Adams, I. M. Shapiro and P. Ducheyne, *J. Biomed. Mater. Res.*, 2004, **71A**, 449–461.
36 J. M. Anderson, N. P. Ziats, A. Azeez, M. R. Brunstedt, S. Stack and T. L. Bonfield, *J. Biomater. Sci., Polym. Ed.*, 1996, **7**, 159–169.
37 M. N. de Silva, R. desai and D. J. Odde, *Biomed. Microdevices*, 2004, **6**, 219–222.
38 E. Leclerc, Y. Sakai and T. Fujii, *Biotechnol. Prog.*, 2004, **20**, 750–755.
39 M.-H. Wu, *Surf. Interface Anal.*, 2009, **41**, 11–16.
40 M. Ni, W. H. Tong, D. Choudhury, N. A. Rahim, C. Iliescu and H. Yu, *Int. J. Mol. Sci.*, 2009, **10**, 5411–5441.
41 K. E. Sapsford and F. S. Ligler, *Biosens. Bioelectron.*, 2004, **19**, 1045–1055.
42 L. Yu, Z. Lu, Y. Gan, Y. Liu and C. M. Li, *Nanotechnology*, 2009, **20**, 285101.
43 T. R. E. Simpson, B. Parbhoo and J. L. Keddie, *Polymer*, 2003, **44**, 4829–4838.
44 S. L. Peterson, A. McDonald, P. L. Gourley and D. Y. Sasaki, *J. Biomed. Mater. Res.*, 2005, **72A**, 10–18.
45 K. Choonee, R. R. A. Syms, M. M. Ahmad and H. Zou, *Sens. Actuators, A*, 2009, **155**, 253–262.
46 D. P. Dowling, C. E. Nwankire, M. Riihimäki, R. Keiski and U. Nylén, *Surf. Coat. Technol.*, 2010, **205**, 1544–1551.

47 A. Zengin and T. Caykara, *Appl. Surf. Sci.*, 2011, **257**, 2111–2117.
48 C. E. Giacomelli and W. Norde, *J. Colloid Interface Sci.*, 2001, **233**, 234–240.
49 W. Norde, *Colloids Surf., B*, 2008, **61**, 1–9.
50 H. Larsericsdotter, S. Oscarsson and J. Buijs, *J. Colloid Interface Sci.*, 2005, **289**, 26–35.
51 N. Hassan, J. M. Ruso and P. Somasundaran, *Colloids Surf., B*, 2011, **82**, 581–587.
52 J. Mayne and J. J. Robinson, *J. Cell. Biochem.*, 2002, **84**, 567–574.
53 S. Dash, S. Mishra, S. Patel and B. K. Mishra, *Adv. Colloid Interface Sci.*, 2008, **140**, 77–94.
54 M. Dion, M. Rapp, N. Rorrer, D. H. Shin, S. M. Martin and W. A. Ducker, *Colloids Surf., A*, 2010, **362**, 65–70.
55 M. F. Mora, C. E. Giacomelli and C. D. Garcia, *Anal. Chem.*, 2009, **81**, 1016–1022.
56 J. L. Felhofer, J. Caranto and C. D. Garcia, *Langmuir*, 2010, **26**, 17178–17183.
57 H. Soetedjo, M. F. Mora and C. D. Garcia, *Thin Solid Films*, 2010, **518**, 3954–3959.
58 J. Wehmeyer, R. Bizios and C. D. Garcia, *Mater. Sci. Eng., C*, 2010, **30**, 277–282.
59 M. F. Mora, M. Reza Nejadnik, J. L. Baylon-Cardiel, C. E. Giacomelli and C. D. Garcia, *J. Colloid Interface Sci.*, 2010, **346**, 208–215.
60 M. R. Nejadnik and C. D. Garcia, *Colloids Surf., B*, 2011, **82**, 253–257.
61 S. A. Alterovitz and B. Johs, *Thin Solid Films*, 1998, **313–314**, 124–127.
62 H. Fujiwara, *Spectroscopic ellipsometry. Principles and applications*, J. Wiley&Sons, West Sussex, England, 2007.
63 R. A. Synowicki, *Thin Solid Films*, 1998, **313–314**, 394–397.
64 M. R. Nejadnik, L. Francis and C. D. Garcia, *Electroanalysis*, 2011, **23**, 1462–1469.
65 S. Logothetidis, M. Gioti, S. Lousinian and S. Fotiadou, *Thin Solid Films*, 2005, **482**, 126–132.
66 D. Filippini, F. Winquist and I. Lundstrom, *Anal. Chim. Acta*, 2008, **625**, 207–214.
67 J. A. D. Feijter, J. Benjamins and F. A. Veer, *Biopolymers*, 1978, **17**, 1759–1772.
68 M. F. Mora, C. E. Giacomelli and C. D. Garcia, *Anal. Chem.*, 2009, **81**, 1016–1022.
69 R. Kurrat, J. E. Prenosil and J. J. Ramsden, *J. Colloid Interface Sci.*, 1997, **185**, 1–8.
70 C. E. Giacomelli, M. J. Esplandiu, P. I. Ortiz, M. J. Avena and C. P. D. Pauli, *J. Colloid Interface Sci.*, 1999, **218**, 404–411.
71 M. Vinnichenko, R. Gago, N. Huang, Y. X. Leng, H. Sun, U. Kreissig, M. P. Kulish and M. F. Maitz, *Thin Solid Films*, 2004, **455–456**, 530–534.
72 S. M. Sirard, H. Castellanos, P. F. Green and K. P. Johnston, *J. Supercrit. Fluids*, 2004, **32**, 265–273.
73 J. C. McDonald and G. M. Whitesides, *Acc. Chem. Res.*, 2002, **35**, 491–499.
74 D. Cai, A. Neyer, R. Kuckuk and H. M. Heise, *J. Mol. Struct.*, 2010, **976**, 274–281.
75 M. A. Hoque, Y. Kakihana, S. Shinke and Y. Kawakami, *Macromolecules*, 2009, **42**, 3309–3315.
76 M. A. Brook, *Silicon in organic, organometallic, and polymer chemistry*, John Wiley and Sons, Inc., New York, 2000.
77 E. P. T. d. Givenchy, S. Amigoni, C. Martin, G. Andrada, L. Caillier, S. Geribaldi and F. Guittard, *Langmuir*, 2009, **25**, 6448–6453.
78 L. E. Valenti, P. A. Fiorito, C. D. Garcia and C. E. Giacomelli, *J. Colloid Interface Sci.*, 2007, **307**, 349–356.
79 R. J. Rapoza and T. A. Horbett, *J. Biomed. Mater. Res.*, 1990, **24**, 1263–1287.
80 B. Verzola, C. Gelfi and P. G. Righetti, *J. Chromatogr., A*, 2000, **874**, 293.
81 M. A. Bos and T. van Vliet, *Adv. Colloid Interface Sci.*, 2001, **91**, 437–471.
82 A. Mackie and P. Wilde, *Adv. Colloid Interface Sci.*, 2005, **117**, 3–13.
83 J. J. Gray, *Curr. Opin. Struct. Biol.*, 2004, **14**, 110–115.
84 V. I. Shcheslavskiy, G. I. Petrov and V. V. Yakovlev, *Chem. Phys. Lett.*, 2005, **402**, 170–174.
85 Z. Adamczyk, J. Barbasz and M. Cieśla, *Langmuir*, 2010, **26**, 11934–11945.
86 A. M. Brzozowska, B. Hofs, A. de Keizer, R. Fokkink, M. A. Cohen Stuart and W. Norde, *Colloids Surf., A*, 2009, **347**, 146–155.
87 C. F. Wertz and M. M. Santore, *Langmuir*, 1999, **15**, 8884–8894.
88 C. F. Wertz and M. M. Santore, *Langmuir*, 2001, **17**, 3006–3016.
89 C. E. Giacomelli and W. Norde, *in Encyclopedia of Surface and Colloid Science*, ed. A. T. Hubbard, Marcel Dekker, New York, 2003.
90 M. M. Santore and C. F. Wertz, *Langmuir*, 2005, **21**, 10172–10178.
91 M. van der Veen, M. C. Stuart and W. Norde, *Colloids Surf. B*, 2007, **54**, 136–142.
92 S. Lousinian, S. Kassavetis and S. Logothetidis, *Diamond Relat. Mater.*, 2007, **16**, 1868–1874.
93 Y. Yu and G. Jin, *J. Colloid Interface Sci.*, 2005, **283**, 477–481.
94 W. Norde*Proteins at Solid Surfaces. Physical Chenistry of Biological Interfaces*, Marcel Dekker, New York, 2000.
95 W. Norde, in *Biopolymers at Interfaces*, ed. M. Malmsten, Marcel Dekker, New York, 2003.